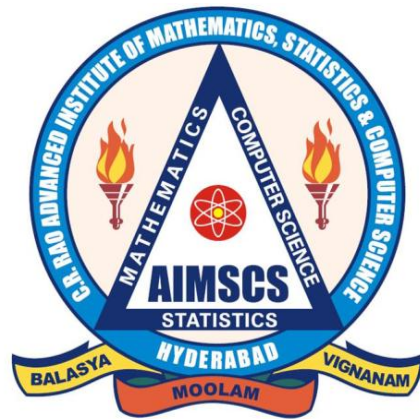


**CRRAO Advanced Institute of Mathematics,  
Statistics and Computer Science (AIMSCS)**

# **Research Report**



**Author (s): Saumyadipta Pyne, Robert Bennett,  
Steven J. Mentzer, et al.**

**Title of the Report: Laser microdissection of the alveolar duct  
enables single-cell genomic analysis**

**Research Report No.: RR2014-13**

**Date: May 15, 2014**

**Prof. C R Rao Road, University of Hyderabad Campus,  
Gachibowli, Hyderabad-500046, INDIA.  
[www.crraoaimscs.org](http://www.crraoaimscs.org)**

# **Laser microdissection of the alveolar duct enables single-cell genomic analysis**

<sup>1</sup>Robert Bennett, <sup>1</sup>Alexandra Ysasi, <sup>1</sup>Janeil Belle, <sup>2</sup>Willi Wagner, <sup>2</sup>Moritz A. Konerding, <sup>3</sup>Paul Blainey, <sup>4</sup>Saumyadipta Pyne\*, <sup>1</sup>Steven J. Mentzer

<sup>1</sup>Laboratory of Adaptive and Regenerative Biology, Brigham & Women's Hospital, Harvard Medical School, Boston, MA, USA.

<sup>2</sup>Institute of Functional and Clinical Anatomy, University Medical Center of the Johannes Gutenberg-University, Mainz, Germany.

<sup>3</sup>Broad Institute of Massachusetts Institute of Technology and Harvard University, Cambridge, MA, USA.

<sup>4</sup>CR Rao Advanced Institute of Mathematics, Statistics and Computer Science, Hyderabad, India.

\*Correspondence: Dr. Saumyadipta Pyne,  
CR Rao Advanced Institute of Mathematics, Statistics and Computer Science,  
University of Hyderabad Campus, Prof. CR Rao Road, Hyderabad - 500046, India.  
spyne@cr Raoaimsres.in

Acknowledgment: The work is supported in part by NIH Grant HL94567. SP is supported by Ramalingaswami-DBT Fellowship, DST CMS (Project No. SR/SA/MS:516/07 dated 21/04/2008) and MoS&PI India.

Abbreviations: 2D, 2-dimensional; 3D, 3-dimensional; IR, infra-red; LCM, laser capture microdissection; PCR, polymerase chain reaction; PEN, polyethylene naphtalene; SEM, scanning electron microscopy; UV, ultraviolet; SCA, Single Cell Analysis

Keywords: Single-cell analysis, laser microdissection, microfluidic arrays, alveolar duct, murine lung, gene expression, signaling network, regenerative medicine.

Running title: Lung single-cell isolation & analysis

## **Abstract**

Complex tissues such as the lung are composed of structural hierarchies such as alveoli, alveolar ducts and lobules. Some structural units, such as the alveolar duct, appear to selectively participate in tissue regeneration. Here, we demonstrate an approach to conduct laser microdissection of the lung alveolar duct for single-cell PCR analysis. Our approach involved three steps. 1) The initial preparation used mechanical sectioning of the lung tissue with sufficient thickness to encompass the structure of interest. In the case of the alveolar duct, the precision-cut lung slices were 200um thick; the slices were processed using near-physiologic conditions to preserve the state of viable cells. 2) The lung slices were examined by transmission light microscopy to target the alveolar duct. The air-filled lung was sufficiently accessible by light microscopy that counterstains or fluorescent labels were unnecessary to identify the alveolar duct. 3) The enzymatic and microfluidic isolation of single cells allowed for the harvest of as few as several thousand cells for PCR analysis. Microfluidics based arrays were used to measure the expression of selected marker genes in individual cells to characterize different cell populations. Preliminary work suggests the unique value of this approach to understanding the intra- and intercellular interactions within the regenerating alveolar duct.

## **Introduction**

Complex tissues such as the lung are composed of structural hierarchies such as alveoli, alveolar ducts and lobules (Weibel and Gomez, 1962). Recent evidence indicates that these structures reflect not only mechanical relationships, but functional units that selectively participate in integrated processes such as tissue regeneration (Weibel, 2008). Since bulk analyses of cells and gene expression—ignoring these distinctive regenerative units—has failed to illuminate the specific interactions among cells participating in these processes (Paxson et al., 2009; Wolff et al., 2009), there is growing interest in the spatial sampling of the cells within regenerative units and studying them systematically.

The initial attempts to refine the bulk analysis of cells within regenerating tissues used flow cytometry (Lin et al., 2011). Flow cytometry is a multi-dimensional high-throughput technology that can analyze and sort individual cells based on their phenotypic characteristics—in most cases, sorting is based on cell surface molecule expression (Zeng et al., 2007; Rossin et al., 2011). This approach has provided useful insights into the molecular expression of cell populations participating in lung regeneration (Chamoto et al., 2012b; Chamoto et al., 2012c; Chamoto et al., 2013a; Chamoto et al., 2013b); nonetheless, the relatively large number of cells sorted by flow cytometry has potentially obscured the cell-cell interactions within individual regenerative units.

To address these limitations, there is growing interest in isolating cells within individual regenerative units; in lung regeneration, the anatomic unit appears to be the alveolar duct. This goal has been aided by two developments. First, computer-controlled laser microdissection of tissue has facilitated the rapid isolation of small anatomic units within complex tissues. The ability to harvest anatomic units, such as the alveolar duct, under physiologic conditions has

enabled detailed single-cell analysis. Second, microfluidic devices capable of capturing and handling single cells allowed for the analysis of the small number of cells comprising anatomic units such as the alveolar duct. Further, these isolated cells can now be analyzed for gene expression at the level of individual cells. The result is an opportunity to define not only the signaling interactions between cells, but also the molecular interactions and signaling pathways within cells (Chamoto et al., 2012b; Konerding et al., 2012; Chamoto et al., 2013a).

In this report, we demonstrate the use of laser microdissection to isolate cells in the murine lung alveolar duct, and the microfluidic isolation and gene expression analysis of individual cells within this structural unit.

## **Materials and Methods**

**Animals.** Male mice, eight to ten week old wild type C57BL/6 (Jackson Laboratory, Bar Harbour, ME, USA) were anesthetized as previously described (Gibney et al., 2011). The care of the animals was consistent with guidelines of the American Association for Accreditation of Laboratory Animal Care (Bethesda, MD, USA) and approved by our Institutional Animal Care and Use Committee.

**Corrosion casting and SEM.** The lung vessels were cannulated and perfused with 15-20ml of 37°C saline followed by a buffered 2.5% glutaraldehyde solution (Sigma, St Louis, MO) at pH 7.40. After casting of the pulmonary microcirculation with PU4ii (VasQtex, Zurich, Switzerland) diluted with 20% methylmethacrylate monomers (Sigma) and caustic digestion, the microvascular corrosion casts were imaged after coating with gold in an argon atmosphere with a Philips ESEM XL30 scanning electron microscope.

**Embedding medium.** Agarose at 30% (w/v) was thoroughly mixed and warmed to 37°C. The trachea was cannulated and the warm agarose infused using the lowest pressure necessary to inflate the peripheral lung. At total lung capacity, the trachea was clamped and the lung block placed in 4°C saline and allowed to harden.

**Precision-cut lung slices.** Sectioning was performed with the Leica VT1000 S vibrating blade microtome (Leica Biosystems, Nussloch, Germany) using stainless steel razor blades (Gillette, Boston, MA). The microtome was operated at the following adjustable settings: knife angle, 5-7°; sectioning speed, 0.05 - 0.2 mm/sec; oscillation frequency, 80-100 Hz; and oscillation amplitude, 0.6 mm. Most sections were 200µm thick and mounted on a polyethylene naphthalene (PEN) membrane frame slide (Life Technologies, Carlsbad, CA).

**Laser microdissection.** The Arturus XT LCM System (Life Technologies) was used for all ultraviolet (UV) laser dissection. The UV laser was a specially adapted beta-test laser for wet tissue applications. The Arcturus XT software was used to target tissue for UV dissection.

**Enzymatic digestion.** Enzymatic digestion of the lung reflected a previously published protocol (van Beijnum et al., 2008). Briefly, collagenase Type IV and DNase I was used to dissociate the tissue. The digestion was performed at 37°C under constant agitation until dissolved. The digest was filtered through 35um nylon mesh in preparation for microfluidic analysis.

**C1 microfluidics chip.** The C1 Single-Cell Auto Prep Array Integrated Fluidic Circuit (chip) is the microfluidic component of the Fluidigm C1™ Single-Cell Auto Prep System. The medium chip (10-17um cell size) was used to capture single cells (96 on one chip) obtained from the laser microdissection. The chip was used to perform single-cell PCR using a custom 96 gene panel designed for the alveolar duct.

**Bioinformatics.** The resulting dataset from the PCR array consists of a matrix of expressions of 96 genes for each of the 96 wells. After a filtering step, we obtained a matrix of 83 genes that show variation in their expressions (given by  $s.d. \geq 1$ ) for 72 single cells as confirmed by QC, i.e., by discarding readouts from wells containing possibly either more than one cell or debris. Sparse hierarchical clustering based on feature selection was performed in the GenePattern platform (available online freely from Broad Institute of MIT) to identify different cell populations defined by the corresponding marker genes.

## Results

**Precision-cut lung slices.** Structural analysis of the murine lung using SEM demonstrated a mean diameter of the intact alveolar duct of  $197 \pm 34 \mu\text{m}$  (Figure 1). To obtain thickness-calibrated lung slices encompassing the alveolar ducts, 200 $\mu\text{m}$  thick precision-cut lung slices were sectioned after intra-airway instillation of a 3% (w/v) agarose embedding medium. At 37°C, low melting point agarose had sufficiently low viscosity to permit instillation into the peripheral airspaces---important for the preservation of alveolar architecture. When cooled to 4°C, the agarose-lung block demonstrated stability for precision sectioning. The agarose-lung block, mounted on Leica VT1000 S specimen holder and immersed in ice-cold PBS, was serial sectioned (Figure 2). For single-cell genomics studies, the lung slices were mounted on a PEN membrane frame slide to provide structural support during laser dissection. The frame slide facilitated the retrieval and subsequent processing of the dissected specimen (Figure 3).

**Optical targeting.** The hierarchical anatomic structure of the lung facilitated the visual identification of the alveolar duct. Although the dehydrated lung lost structural features by light microscopy, the well-hydrated lung was readily examined throughout the 200-300 $\mu\text{m}$  depth in the precision-cut lung slices in the absence of counterstains or cell-specific labels (Figure 4). Preliminary identification of the alveolar duct was confirmed by varying the optical plane and identifying the feeding bronchiole (Figure 4A,B). The computer-controlled laser software allowed for precise selection of regions encompassing the alveolar duct; the demarcated regions were harvested by the UV cutting laser (Figure 4C,D). The laser power, speed and focal point was varied to optimize single-pass dissection of the tissue and minimize thermal damage. The required laser power was consistently reduced by 50% with absorbent blotting of the section surface followed by re-application of media immediately following UV dissection.

**Single-cell isolation.** The laser-dissected samples were enzymatically digested, microfiltered and prepared for microfluidic analysis (Figure 5). The PEN membrane-associated samples were incubated in collagenase Type IV buffer for 15-30 minutes at 37°C with constant agitation. The acellular matrix and PEN membrane-associated debris were microfiltered with a 30um mesh. Cell yields varied from 1-3x10<sup>3</sup> cells per alveolar duct. Cell viabilities ranged from 70-90% depending upon treatment conditions. The cells were analyzed using the Fluidigm C1™ Single-Cell Auto Prep System (Fluidigm, South San Francisco, CA). In the 96 well C1 system, a typical result was the capture of 75 single cells, 13 wells with 2 or more cells and 2 wells with no cells.

**Single-cell PCR.** The C1 chip used a microfluidic circuit to capture the isolated single cells (96 on one chip). The single cell poly-adenylated RNA was converted to full-length cDNA for universal amplification of the cDNA and custom PCR analysis. Our custom PCR arrays were developed based on gene expression studies using flow cytometry-based phenotypic isolation of lung cells (Chamoto et al., 2011;Lin et al., 2011;Chamoto et al., 2012a;Chamoto et al., 2012c;Chamoto et al., 2013a;Chamoto et al., 2013b). Results of the C1 PCR studies were analyzed by unsupervised hierarchical clustering (Figure 6). Clustering based on selected features demonstrated single-cell clusters (Figure 7) that corresponded to previously identified cell types (e.g. endothelial cells, myofibroblasts and macrophages). Gene expression clusters likely reflect cell-specific signaling modules.

## Discussion

In this report, we demonstrated laser microdissection of the lung alveolar duct for single-cell PCR analysis. Our approach involved three steps. 1) The initial preparation used mechanical sectioning of the lung tissue with sufficient thickness to encompass the structure of interest. In the case of the alveolar duct, the precision-cut lung slices were 200um thick and processed using near-physiologic conditions to preserve cell viability. 2) The lung slices were examined by transmission light microscopy to target the alveolar duct. The air-filled lung was sufficiently accessible by light microscopy that counterstains or fluorescent labels were unnecessary to identify the alveolar duct. 3) The enzymatic and microfluidic isolation of single cells for PCR allowed for the harvest of as few as several thousand cells for analysis. The data suggest the unique value of this approach to understanding the intra- and intercellular interactions within the regenerating or neoplastic alveolar duct.

Harvesting viable cells from the alveolar duct requires that tissue slices of the appropriate thickness be obtained in near-physiologic conditions. Manually sliced tissues have been used for nearly 90 years in various *in vitro* applications (Warburg, 1923;Graaf et al., 2007); however, the manually prepared slices have had limited reproducibility and viability (Olinga et al., 1998). A mechanical tool to facilitate the cutting of tissue of precise thickness was introduced by the Krumdieck in 1980 (Krumdieck et al., 1980;Krumdieck, 2013). With progressive refinement, tissue microtomes now vibrate with varying amplitudes and frequencies to produce slices with highly reproducible thickness—thus, these sections are referred to as precision-cut tissue slices (Morin et al., 2013). With current vibrating microtomes, precision-cut tissue slices preserve the original organ architecture, the cellular heterogeneity and extracellular matrix found *in vivo* (Fahy et al., 2013). Precision-cut tissue slices, for example, have enabled the development of ex

vivo systems for systematic pharmaco-kinetic profiling of tumors contained in their native 3-dimensional micro-environment (Vaira et al., 2010).

A key feature of precision-cut lung slices in the lung is the use of agarose as structural support. Because live tissue is too soft for precise sectioning, and molten paraffin is too hot for live tissue, a biocompatible liquid with a low-temperature gelling point is used as an embedding medium. Agarose is typically used for lung embedding because it has sufficiently low viscosity at 37-40°C to be infused into the distal airspaces, yet is sufficiently rigid for microtome sectioning at 4°C.

Although there is significant overlap between techniques, laser microdissection can be distinguished from laser capture microdissection (LCM) by the method of cell isolation. In the original LCM system developed at the National Institutes of Health, the target cells were identified by light microscopy and captured using an infrared laser (Emmert-Buck et al., 1996). A transfer film positioned over the region of interest (typically tumor cells) was melted into the tissue using an IR laser. The dissected tissue microsample was then lifted from the histopathology slide for subsequent RNA, DNA or protein analysis. In most contemporary LCM systems, a requirement for effective capture is the dehydration of the tissue—a requirement that precludes the study of live cells (Vandewoestyne et al., 2013). In contrast, our laser microdissection approach uses a cutting ultraviolet (UV) laser to define the margins of the dissection under near-physiologic conditions. Although UV-induced thermal injury to the neighboring cells is demonstrable using live-dead assays; the dissection margins can be drawn to minimize the injury to the region of interest. In our application, we maintained near-physiologic conditions during the UV laser dissection with only blotting of the tissue surface to minimize excess liquid media prior to UV dissection. The UV laser-defined alveolar duct was

subsequently transferred to the collection chamber without the use of an IR laser or transfer film; in most cases, the sample dropped into the chamber occasionally assisted by the application of liquid media.

A frequently under-appreciated characteristic of the lung is the large amount of extracellular matrix in the organ (Badylak, 2007). In addition, some extracellular matrix components—most notably, elastin—are resistant to common enzymatic treatments (Duca et al., 2004). In our application, we have used a variety of enzymatic cocktails based on collagenase to facilitate dissolution of the laser-dissected tissue; however, the most important component has proven to be collagenase Type IV. In our protocols, we used 30um mesh to separate cells from the collagenase-resistant matrix debris. Routine re-examination of the filtered debris did not show residual cells suggesting that this approach does not result in the systematic loss of any particular cell subpopulation. Of note, cell filtration with mesh larger than 30um was prone to debris-induced occlusion of the microfluidics chip.

The cells isolated by microfluidics were studied using a custom 96 gene PCR panel. The results of prior flow cytometry population studies were used to select the genes used in this custom panel (Chamoto et al., 2011; Lin et al., 2011; Chamoto et al., 2012a; Chamoto et al., 2012c; Chamoto et al., 2013a; Chamoto et al., 2013b). Flow cytometry-derived cell type-specific markers were incorporated into the panel to facilitate the spatial reconstruction of intercellular interactions within the alveolar duct. For example, the genes *Actin2* and *Pecam1* were added to the PCR panel to identify myofibroblasts and endothelial cells, respectively. Although the single-cell transcriptional data must be analyzed in the context of potential limitations, such as burst transcription (Livak et al., 2013; Wills et al., 2013), insights derived from these data should be useful for re-interpreting population-based data both *in vivo* and *in vitro*.

Finally, these results demonstrate the ability to extract viable cells from a morphologically-defined micro-region of a tissue sample. We successfully applied single-cell whole-transcriptome amplification and gene expression analyses to these sample—a process which allows for simultaneous region-specific and cell type-specific expression analysis. We anticipate even more interesting experiments are possible in the future. For example, similarly obtained viable single cells can facilitate a variety of experimental perturbations prior to endpoint analyses (e.g. expression profiling, nucleic acid sequencing, immunoassays, or proteomics). Further, new statistical and bioinformatics techniques may be used to design efficient strategies for sampling cells at different locations in the tissue and at different time-points, and to study the genomic and transcriptomic signals by taking into consideration the cell-to-cell stochastic variation, overall heterogeneity and platform noise, thus leading to construction of robust and insightful spatio-temporal cell signaling networks. We are confident that such single-cell analysis studies will lead to a more nuanced understanding of the process of tissue regeneration.

## Figure Legends.

**Figure 1.** Scanning electron microscopy (SEM) of the polymer casted murine lung. Vascular fixation and casting—the method with the least shrinkage of common lung preparation techniques—demonstrated bronchiolar and aveolar duct architecture when examined by SEM. The alveolar ducts were demonstrably contained within the 200um tissue slice.

**Figure 2.** Precision-cut lung slices were obtained by a vibrating blade microtome after agarose embedding (A). The agarose-lung block was initially mounted on a cork specimen platform with cyanoacrylate prior to sectioning (inset). The cut sections were subsequently mounted on a frame slide with a PEN membrane used for standard laser capture microdissection (B).

**Figure 3.** The tissue slice was mounted on a frame slide. The slide is composed of a standard optical microscope slide with a metal frame that supports a PEN membrane to facilitate laser microdissection (a). In cross-section (b), the frame slide creates a reservoir for retrieval of the dissected tissue.

**Figure 4.** Lung slices of the murine cardiac lobe examined by light microscopy. After mounting on a frame slide, the sections were visualized without counter-stain at 10x (A,C,D) and 20X (B) magnification. The respiratory bronchiole and alveolar ducts were readily identified (B). The relevant anatomic structure was demarcated by software annotation (C) and laser microdissected using computer control (D). Successful dissection is demonstrated as the structure drops into the frame slide and out of the optical plane (D).

**Figure 5.** Schematic of the single-cell isolation procedure after laser microdissection. The tissue samples were enzymatically digested and microfiltered using a 30um mesh. Single cells were isolated and PCR performed on a C1 microfluidics chip. The successful capture of individual cells was readily identified by light microscopy (inset, small arrow).

**Figure 6.** The gene expression data matrix for 96 SCA samples, each assayed for 96 genes from the custom PCR panel, was clustered using an unsupervised hierarchical clustering algorithm. Phenotypic "markers" were incorporated into the gene expression panel to facilitate cell subset identification as well as to correspond with the histologic and the flow cytometric studies. Four groups of markers significantly expressed at single-cell level are shown (top dendrogram).

**Figure 7.** After filtering of PCR data (see Methods), sparse hierarchical clustering of 72 confirmed single-cells was performed. The different cell populations based on the selected features – 42 marker genes – are shown (top dendrogram). Marker-specific variation is indicated by standard deviation (denoted by s.d.).

## References

- Badylak, S.F. (2007). The extracellular matrix as a biologic scaffold material. *Biomaterials* 28, 3587-3593 doi:10.1016/j.biomaterials.2007.04.043
- Chamoto, K., Gibney, B., Lin, M., Lee, G.S., Collings-Simpson, D., Houdek, J., Konerding, M.A., Tsuda, A., and Mentzer, S.J. (Year). "Regulatory network of angiogenesis gene expression during post-pneumonectomy compensatory growth", in: *American Thoracic Society*).
- Chamoto, K., Gibney, B.C., Ackermann, M., Lee, G.S., Konerding, M.A., Tsuda, A., and Mentzer, S.J. (2012a). Alveolar epithelial dynamics in post-pneumonectomy lung growth. *Anat. Rec.* 296, 496-503
- Chamoto, K., Gibney, B.C., Ackermann, M., Lee, G.S., Konerding, M.A., Tsuda, A., and Mentzer, S.J. (2013a). Alveolar Epithelial Dynamics in Postpneumonectomy Lung Growth. *Anat. Rec.* 296, 495-503 doi:10.1002/ar.22659
- Chamoto, K., Gibney, B.C., Ackermann, M., Lee, G.S., Lin, M., Konerding, M.A., Tsuda, A., and Mentzer, S.J. (2012b). Alveolar macrophage dynamics in murine lung regeneration. *J. Cell. Physiol.* 227, 3208-3215
- Chamoto, K., Gibney, B.C., Lee, G.S., Ackermann, M., Konerding, M.A., Tsuda, A., and Mentzer, S.J. (2013b). Migration of CD11b+ accessory cells during murine lung regeneration. *Stem Cell Res.* 10, 267-277
- Chamoto, K., Gibney, B.C., Lee, G.S., Lin, M., Simpson, D.C., Voswinckel, R., Konerding, M.A., Tsuda, A., and Mentzer, S.J. (2012c). CD34+ progenitor to endothelial cell transition in post-pneumonectomy angiogenesis. *Am. J. Resp. Cell Mol. Biol.* 46, 283-289
- Duca, L., Floquet, N., Alix, A.J.P., Haye, B., and Debelle, L. (2004). Elastin as a matrikine. *Crit. Rev. Oncol./Hematol.* 49, 235-244 doi:10.1016/j.critrevonc.2003.09.007
- Emmert-Buck, M.R., Bonner, R.F., Smith, P.D., Chuaqui, R.F., Zhuang, Z., Goldstein, S.R., Weiss, R.A., and Liotta, L.A. (1996). Laser capture microdissection. *Science* 274, 998-1001
- Fahy, G.M., Guan, N., De Graaf, I.a.M., Tan, Y., Griffin, L., and Groothuis, G.M.M. (2013). Cryopreservation of precision-cut tissue slices. *Xenobiotica* 43, 113-132 doi:10.3109/00498254.2012.728300
- Gibney, B., Lee, G.S., Houdek, J., Lin, M., Chamoto, K., Konerding, M.A., Tsuda, A., and Mentzer, S.J. (2011). Dynamic determination of oxygenation and lung compliance in murine pneumonectomy. *Exp. Lung Res.* 37, 301-309

- Graaf, I.a.M., Groothuis, G.M.M., and Olinga, P. (2007). Precision-cut tissue slices as a tool to predict metabolism of novel drugs. *Expert Opin. Drug Metab. Toxicol.* 3, 879-898 doi:10.1517/17425255.3.6.879
- Konerding, M.A., Gibney, B.C., Houdek, J., Chamoto, K., Ackermann, M., Lee, G., Lin, M., Tsuda, A., and Mentzer, S.J. (2012). Spatial dependence of alveolar angiogenesis in post-pneumonectomy lung growth. *Angiogenesis* 15, 23-32
- Krumdieck, C.L. (2013). Development of a live tissue microtome: reflections of an amateur machinist. *Xenobiotica* 43, 2-7 doi:10.3109/00498254.2012.724727
- Krumdieck, C.L., Dossantos, J.E., and Ho, K.J. (1980). A new instrument for the rapid preparation of tissue-slices. *Anal. Biochem.* 104, 118-123 doi:10.1016/0003-2697(80)90284-5
- Lin, M., Chamoto, K., Gibney, B., Lee, G.S., Collings-Simpson, D., Houdek, J., Konerding, M.A., Tsuda, A., and Mentzer, S.J. (2011). Angiogenesis gene expression in murine endothelial cells during post-pneumonectomy lung growth. *Resp. Res.* 12:98
- Livak, K.J., Wills, Q.F., Tipping, A.J., Datta, K., Mittal, R., Goldson, A.J., Sexton, D.W., and Holmes, C.C. (2013). Methods for qPCR gene expression profiling applied to 1440 lymphoblastoid single cells. *Methods* 59, 71-79 doi:10.1016/j.ymeth.2012.10.004
- Morin, J.P., Baste, J.M., Gay, A., Crochemore, C., Corbiere, C., and Monteil, C. (2013). Precision cut lung slices as an efficient tool for in vitro lung physio-pharmacotoxicology studies. *Xenobiotica* 43, 63-72 doi:10.3109/00498254.2012.727043
- Olinga, P., Meijer, D.K.F., Slooff, M.J.H., and Groothuis, G.M.M. (1998). Liver slices in in vitro pharmacotoxicology with special reference to the use of human liver tissue. *Toxicol. In Vitro* 12, 77-100 doi:10.1016/s0887-2333(97)00097-0
- Paxson, J.A., Parkin, C.D., Iyer, L.K., Mazan, M.R., Ingenito, E.P., and Hoffman, A.M. (2009). Global gene expression patterns in the post-pneumonectomy lung of adult mice. *Respir Res* 10, 1-15
- Rossin, E., Lin, T.-I., Hsiu, J.H., Mentzer, S.J., and Pyne, S. (2011). A framework for analytical characterization of monoclonal antibodies based on reactivity profiles in different tissues. *Bioinformatics* 27, 2746-2753
- Vaira, V., Fedele, G., Pyne, S., Fasoli, E., Zadra, G., Bailey, D., Snyder, E., Favarsani, A., Coggi, G., Flavin, R., Bosari, S., and Loda, M. (2010). Preclinical model of organotypic culture for pharmacodynamic profiling of human tumors. *Proc. Natl. Acad. Sci. U. S. A.* 107, 8352-8356 doi:10.1073/pnas.0907676107
- Van Beijnum, J.R., Rousch, M., Castermans, K., Van Der Linden, E., and Griffioen, A.W. (2008). Isolation of endothelial cells from fresh tissues. *Nat. Protoc.* 3, 1085-1091 doi:10.1038/nprot.2008.71

- Vandewoestyne, M., Goossens, K., Burvenich, C., Van Soom, A., Peelman, L., and Deforce, D. (2013). Laser capture microdissection: Should an ultraviolet or infrared laser be used? *Anal. Biochem.* 439, 88-98 doi:10.1016/j.ab.2013.04.023
- Warburg, O. (1923). Versuche an uberlebendem karzinomgewebe. *Biochem. Z.* 142, 317-333
- Weibel, E.R. (2008). How to make an alveolus. *Eur. Respir. J.* 31, 483-485 doi:10.1183/09031936.00003308
- Weibel, E.R., and Gomez, D.M. (1962). Architecture of the human lung. *Science* 137, 577-585
- Wills, Q.F., Livak, K.J., Tipping, A.J., Enver, T., Goldson, A.J., Sexton, D.W., and Holmes, C. (2013). Single-cell gene expression analysis reveals genetic associations masked in whole-tissue experiments. *Nat. Biotechnol.* 31, 748-753 doi:10.1038/nbt.2642
- Wolff, J.C., Wilhelm, J., Fink, L., Seeger, W., and Voswinckel, R. (2009). Comparative gene expression profiling of postnatal and post-pneumonectomy lung growth. *Eur. Respir. J.* 28, 28
- Zeng, Q.T., Pratt, J.P., Pak, J., Ravnic, D., Huss, H., and Mentzer, S.J. (2007). Feature-guided clustering of multi-dimensional flow cytometry datasets. *J. Biomed. Inform.* 40, 325-331 doi:10.1016/j.jbi.2006.06.005